Ultrasound Modulated Light Blood Flow Measurement using Intensity Autocorrelation Function - A Monte-Carlo Simulation

A. Tsalach[a], Y. Metzger[a], I. Breskin[a], R. Zeitak[a], R. Shechter[a1]
[a] Ornim Medical Ltd, Israel

ABSTRACT

Development of techniques for continuous measurement of regional blood flow, and in particular cerebral blood flow (CBF), is essential for monitoring critical care patients. Recently, a novel technique, based on ultrasound modulation of light was developed for non-invasive, continuous CBF monitoring (termed ultrasound-tagged light (UTL or UT-NIRS)), and shown to correlate with readings of 133 Xe SPECT[1] and laser Doppler[2]. Coherent light is introduced into the tissue concurrently with an Ultrasound (US) field. Displacement of scattering centers within the sampled volume induced by Brownian motion, blood flow and the US field affects the photons' temporal correlation. Hence, the temporal fluctuations of the obtained speckle pattern provide dynamic information about the blood flow. We developed a comprehensive simulation, combining the effects of Brownian motion, US and flow on the obtained speckle pattern. Photons trajectories within the tissue are generated using a Monte-Carlo based model. Then, the temporal changes in the optical path due to displacement of scattering centers are determined, and the corresponding interference pattern over time is derived. Finally, the light intensity autocorrelation function of a single speckle is calculated, from which the tissue decorrelation time is determined. The simulation's results are compared with *in-vitro* experiments, using a digital correlator, demonstrating decorrelation time prediction within the 95% confidence interval. This model may assist in the development of optical based methods for blood flow measurements and particularly, in methods using the acousto-optic effect.

Keywords: Blood Flow, Acousto-Optic, Simulation

1. INTRODUCTION

The vital need for a continuous, bed-side, reliable method for measuring cerebral blood flow (CBF) non-invasively drives the development of various techniques and devices.

Optical based techniques, involving analysis of dynamic light scattering, provide a promising approach for noninvasive evaluation of blood flow. However, existing methods such as Diffuse Correlation Spectroscopy (DCS) and Laser Doppler suffer each from its own drawbacks, such as shallow sampling volumes and low signal to noise ratio[3, 4]. We have demonstrated a novel non-invasive method for blood flow measurement based on light scattering and the acousto-optic effect, named Ultrasound Tagged Light (UTL)[2]. This is a hybrid technique which combines ultrasonic resolution with optical contrast, thus suggesting better spatial resolution while relying on the optical properties of the tissue. Coherent light is introduced into the tissue together with an Ultrasound (US) field. Displacement of scattering centers within the sampled volume induced by Brownian motion, blood flow and the US field affects the photons' temporal correlation. Hence, the temporal fluctuations of the obtained speckle pattern provide dynamic information about the blood flow. To achieve better understanding of the related phenomena and a quantitative analysis of the blood flow signal, an accompanying computerized simulation is required.

Monte-Carlo simulations are commonly used to model light propagation within a turbid media in general, and in tissue in particular[5-7]. Their inherent advantages over analytical methods, such as enabling the work with complicated geometries and providing quantitative information as to the optical paths, make them an especially valuable tool in tissue optics. At the beginning, these simulations mainly dealt with transmission and reflectance of light and the generation of a speckle pattern in a steady state, without an analysis of the speckle temporal fluctuations. Dynamic investigation of the speckle

[1]Correspondence to R. Shechter, Ph.D.: E-mail Revital@ornim.com

Photons Plus Ultrasound: Imaging and Sensing 2014, edited by Alexander A. Oraevsky, Lihong V. Wang,
Proc. of SPIE Vol. 8943, 89433N · © 2014 SPIE · CCC code: 1605-7422/14/$18 · doi: 10.1117/12.2037246

properties was only later demonstrated for several specific situations, i.e. the effect of blood flow[8-12] or US[13-16] on the obtained light intensity signal.
The influence of blood flow on backscattered light was modeled mostly for Laser Doppler purposes[8-12], and was utilized to evaluate and optimize different detection parameters (e.g. source-detector distance, detector geometry, light wavelength, etc). Thus, the simulations usually analyzed changes of the intensity spectrum, to identify phase shifts induced by moving particles, rather than deal with the temporal behavior of intensity autocorrelation function. It has been shown that blood flow parameters, such as velocity magnitude and the concentration of moving blood cells, can be determined from the spectrum of the detected intensity fluctuations[17]. Yet, the effects of other motions, such as Brownian motion or motion induced by US, were not discussed. A further dynamic analysis was provided by Boas et al.[18], who modeled light propagation under the influence of either spatially uniform Brownian motion or spatially uniform random flow, but did not combine them both.
Ultrasonic modulation of multiply scattered coherent light was extensively modeled by Wang *et al.*[13-16]. They described the influence of US on light transport with some references to Brownian motion, however they did not utilize the technique for blood flow measurement, therefore no association with flow was suggested. Lev et al.[19], in comparison, had derived an analytic model that integrates the influence of US modulation along with scatterers displacement due to Brownian or other external (such as biological) motion, and investigated the speckle fluctuations of the US modulated light signal. Yet, their examination included development of an analytic model and its validation in *in-vitro* and *in-vivo* experiments only, with no computerized simulation to support it.
To the best of our knowledge, until today no simulation which combines the influence of US, blood flow and Brownian motion exists. This work presents a comprehensive simulation that considers the contribution of all the above mentioned movements and investigates the overall influence on the obtained signal. It is further examined in *in-vitro* experiments, validating the simulation model and its ability to predict actual temporal behavior of intensity autocorrelation functions in the presence of Brownian motion. Such a simulation may be extremely valuable and assist in the development of optical based methods for blood flow measurements and particularly, in methods using the acousto-optic effect.

2. METHODS

2.1 Computerized Simulation

Our simulation models a light point source, perpendicularly illuminating a semi-infinite, highly scattering medium (the tissue), with known optical properties. We assume the tissue slab is much wider than the spatial extent of the photon distribution, therefore the tissue is considered to be infinitely wide. The tissue consists of non-interacting spherical Rayleigh scatterers (see example of TiO_2 below). The back reflected photons are collected by a $2mm \times 4mm$ detector, located at a predetermined distance from the source. The simulation can be practically divided into two consecutive complementary parts. The first is generation of photon trajectories within the tissue, and the second includes modifying the photon paths according to the scatterers' motion induced by the three different mechanisms, i.e. Brownian motion, flow and US, and investigating the obtained intensity signals and their autocorrelation functions.
A Monte-Carlo (MC) simulation was utilized to produce the photon trajectories within the tissue. The simulation's inputs are the source-detector distance and the medium properties (anisotropy - g, scattering coefficient - μ_s, and absorption coefficient - μ_a) and its output is a list of photon paths. Generation of a single photon trajectory initiates with drawing the step size between two consecutive scattering events, using μ_s and an exponential distribution (according to Beer-Lambert law). Then, the scattering angle is established using Henyey-Greenstein function[20] and the new direction of progress is defined. This process is repeated until the photon exits the tissue at the detector face. Trajectories that don't reach the detector are neglected.
Given the obtained trajectories, the expected light intensity at the detector is calculated over time. The different motions within the medium (US, Brownian motion, blood flow) give rise to scatterers' displacement and change the optical path of the photons. The different interference between these paths causes changes in the light intensity over time so that an autocorrelation function can be calculated.
As mentioned, photon trajectories are selected using a statistical approach (MC). With this approach trajectories are determined by selection of random parameters according to known probability functions. If we refer to a set of trajectories at a single time as composing a "speckle", then for two consecutive time points, we shall get totally different speckle patterns due to the random nature of trajectory selection. However, since we are interested in the intensity

autocorrelation function, as different speckles are uncorrelated, correlations can only occur because of the change of intensity in the "same" speckle. Hence, we select a set of trajectories once, and study the intensity changes induced by this set throughout the whole simulation. The simulated motion produces a change in the positions of the trajectory scatterers, while keeping the identity of the trajectories during their deformation. Practically, we pair each trajectory at time 0 with a trajectory at time t that consists of the same scatterers in the same order. As shown in Figure 1, the scatterers have moved, so the optical path has changed, but the difference in phase is probably small and is due to the actual motion and not to selection of a different trajectory.

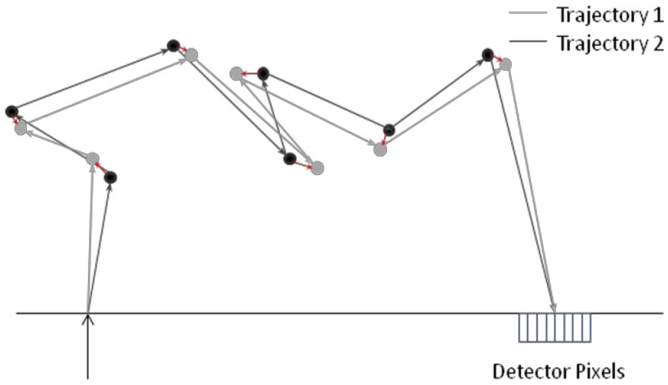

Figure 1: Path deformation due to scatterers' displacement

Note that it is not clear that the "perturbed" trajectory is indeed a true trajectory. When deforming a trajectory it is possible that new scatterers move into the path and occlude the photons. If this happens, it is incorrect to include this deformed trajectory. However, since the typical distance between non participating scatterers and our selected trajectory are of the order of the mean distance between scatterers, we can ignore this phenomenon for the short time scales (under 1nsec) we are dealing with.

The intensity at the detector is defined by

$$I = \left| \sum_{\alpha} A_{\alpha} \right|^2 \tag{1.1}$$

where A_α is the amplitude obtained by trajectory α and given by

$$A_\alpha = W_\alpha e^{-i\phi_\alpha} \tag{1.2}$$

here, W_α denotes the weight and "absorption" behavior of the path, and ϕ_α represents the phase due to the optical path, which changes with time due to the scatterers' motion.

The weight W_α, is a function of the trajectory properties and taken into account in the MC simulation. Due to the use of the Henyey-Greenstein function, the generated trajectories are, in fact, already weighted. More probable trajectories will appear more times, thus we do not have to attach a specific weight to each trajectory.

As for the ϕ_α's, using the trajectories provided by the MC simulation, we could in principle calculate the optical path of each trajectory. However, since we wish to use these ϕ_α's in the autocorrelation calculation, we are actually only interested in their changes over time. Hence, we may treat each ϕ_α as a sum of an initial random phase, and a phase increment, which is due to the deformation of the trajectory, and produces small changes in this value. We can write (for small deformations):

$$\phi_\alpha(t) = \phi_\alpha(0) + \Delta\phi_\alpha \tag{1.3}$$

where,

$$\Delta\phi_\alpha = \sum_{i=1}^{N} Q_i \cdot \Delta\vec{r}_i \tag{1.4}$$

Q_i represents the k vector difference between consecutive scattering events (i and i+1) of the optical path, and $\Delta\vec{r}_i$ represents the position change of the i-th scatterer due to the motion within the tissue[19]. N is the number of scatterers in trajectory α.
Therefore, we need to estimate the phase increment obtained by each trajectory over time and sum up the overall interference at the detector. This will yield the light intensity at the detector, from which the autocorrelation function (ACF) is calculated using equation (1.5):

$$ACF(\tau) = \int_{-\infty}^{\infty} I(t+\tau) I(t)\, dt \tag{1.5}$$

τ denotes the time delay of the autocorrelation function.
The overall process is summed up in the flow chart below:

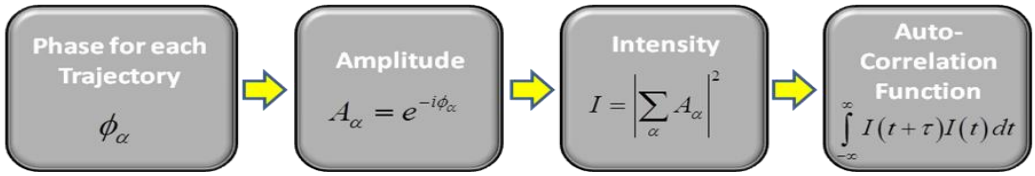

For each motion type the trajectory phase changes differently with time and is given by a different expression:

Brownian motion - the scatterers motions are modeled by a random walk with a step size which is dependent upon the medium's diffusion coefficient. It is therefore described by the following expression (using Fick's law of diffusion):

$$\Delta\phi_{\alpha,diff} = \sum_{i=1}^{N} Q_i \cdot \sqrt{6Dt} \cdot \hat{\eta}_i \tag{1.6}$$

Where D $[m^2/\text{sec}]$ denotes the medium diffusion coefficient, t [sec] is the time step between two sampling consecutive points, and $\hat{\eta}_i$ is a unit variance Gaussian random vector that indicates the scatterer's progress direction. A calculation assuming Q_i's with $\langle Q_x^2 \rangle = 0.25$, which will not be detailed here, yields the corresponding autocorrelation function presented in the following expression:

$$ACF_{diff}(\tau) \sim e^{-6N|k|^2 D\tau/4} \tag{1.7}$$

Here, k is the wave number of light. Given that autocorrelation function, we expect to observe an exponential decay in time.

Continuous ultrasound - Several mechanisms for light modulation by US were proposed in the literature[21-24]. Such mechanisms are displacement of optical scatterers, modulation of the refraction index, and ultrasound-induced variations of the optical properties. The first two are coherent phenomena, thus require the use of coherent light in order to be noticed, while the latter doesn't. As mentioned before, we focus on scatterers' displacement that contribute to the phase increment, thus we model only the first mentioned mechanism for US modulation.
Assuming that a continuous sinusoidal US field is applied to the tissue, its effect on the scatterers is modeled by periodical motion in its central frequency along the transmission axis (z). It is therefore described by the following expression:

$$\Delta\phi_{\alpha,US} = \sum_{i=1}^{N} Q_i \cdot U_0 \sin\left(\omega t + \varphi_i(z)\right) \cdot \hat{z} \tag{1.8}$$

where U_0 is the scatterer displacement maximal amplitude due to the applied US field (taken from the literature[25]), $\omega = 2\pi f$ is the US angular frequency, and φ_i is the US phase for the i-th scatterer. The US field has a different phase for each scatterer due to its different position along the z axis ("sees" the US with a different delay). $\hat{z}$ is a unit vector in the z direction to represent a displacement along the US propagation axis. The corresponding autocorrelation function would be:

$$ACF_{US}(\tau) \sim e^{-U_0^2|k|^2 N(1-\cos(\omega\tau))} \tag{1.9}$$

This function is expected to exhibit an oscillating behavior.

Blood flow - for simplicity, we modeled flow in one direction only (parallel to the tissue surface – y direction). The extension to a general flow direction is straight forward. Assuming flow with a constant velocity amplitude V, the phase expression over time is given by

$$\Delta\phi_{\alpha,\,flow} = \sum_{i=1}^{N} p_i Q_i \cdot Vt \cdot \hat{y} \tag{1.10}$$

where $\hat{y}$ is a unit vector, and p_i is a binary parameter which indicates whether the i-th scatterer is moved by the flow or not. The corresponding autocorrelation function would be:

$$ACF_{flow}(\tau) \sim e^{-\zeta N|k|^2 V^2 \tau^2} \tag{1.11}$$

Where ζ is the fraction of scatterers that actually participate in the flow. Therefore we would expect to observe a Gaussian decay in time.

Our simulation was set to model a previously described tissue phantom[26], comprised from Glycerol and TiO_2 (scattering particles). This phantom was proved to mimic tissue for both optical and ultrasonic properties. Therefore, the Monte-Carlo simulation was fed with the following values: d=9mm (source-detector distance), g=0.55[27], $\mu_s = 25cm^{-1}$ [26] (for 0.1% TiO_2), and $\mu_a = 0cm^{-1}$. Important to mention that since we concentrate on flow measurements and assessment, the phantom's absorbance is irrelevant (hence was selected as zero), and the scattering properties are the most significant ones. This phantom was later used in the *in-vitro* validation.

2.2 *In-Vitro* Experiments

In order to validate our simulation in an *in-vitro* experiment, we evaluated its performance in decorrelation time prediction in solutions with various Brownian motion characteristics. We used H_2O-Glycerol solutions with several different compositions, and set the simulation to model Brownian motion only. To generate a single prediction by the simulation, we determined the expected diffusion coefficient of the solution, by the H_2O-Glycerol composition (which yields the solution's viscosity) and Einstein-Stocks equation:

$$D = \frac{K_B T}{6\pi R\eta} \tag{1.12}$$

where K_B is the Boltzman constant, T is the solution temperature, R is the scatterers' radius (assuming spherical scatterers), and η is the dynamic viscosity of the solution, which was obtained from the literature[28]. To verify the literature values, several solutions' viscosities were validated using a viscometer (Cannon-Fenske Routine viscometer). R (scatterers' radius) was estimated using a microscope and set on 1 micron. The obtained diffusion coefficient was supplied to the simulation to establish the expected intensity autocorrelation function. We later compared this function to an *in-vitro* measurement of the autocorrelation function obtained by a correlator (in a setup that is described next).

Experimental Setup:
The experimental setup[19] is shown in Figure 2. Light from a long coherence length (>1m), 785nm wavelength laser diode was coupled to a 62.5μm multi mode fiber. This fiber was then inserted into a phantom with variable glycerol concentration. The scattering particles concentration remained constant (0.1% Titanium Dioxide (TiO_2)). Another, 9μm single mode fiber, was inserted to the phantom, 9mm away from the transmission fiber. This receiving fiber collected light from the phantom and redirected it towards a Single Photon Counting Module (SPCM ALV/SO-SIPD). The signal detected by the SPCM was sent to a digital correlator board (ALV-5000) to generate the intensity autocorrelation function.

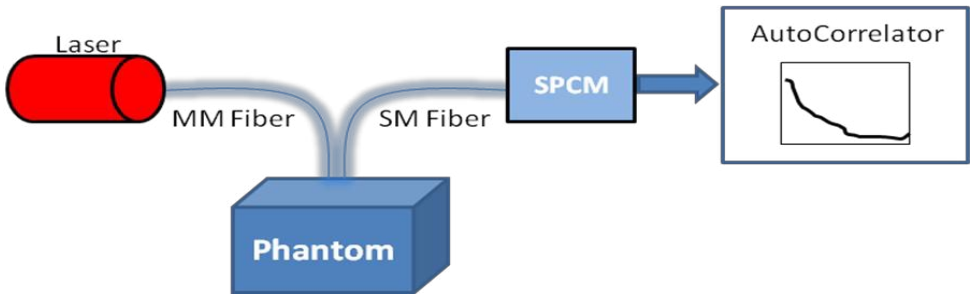

Figure 2: Experimental setup for the *in-vitro* validation experiment. The phantom is illuminated using a 785nm laser diode through a multi-mode fiber. The light is then collected using a single-mode fiber and delivered to a single photon counting module (SPCM) that sends the signal to a digital correlator, which provides the intensity autocorrelation function.

Phantom preparation:
Our goal was to alter the phantom's viscosity, thereby altering its diffusion coefficient and the corresponding decorrelation time, while maintaining constant scattering properties. Thus, two sets of solutions were produced, both containing 1gr of TiO_2 particles (scattering centers (Sigma Aldrich)) but each consisting of different type of liquid solvent, either 1 liter of glycerol or 1 liter of H_2O. The mixtures were vigorously stirred until a uniform solution was obtained. To establish a series of solutions with various viscosities, different combinations of the two solutions were prepared. It is important to note that any combination of these two solutions will maintain a scatterers' concentration of 0.1% TiO_2 (by weight). Therefore, the scattering properties of the generated solutions are assumed to remain similar, and the expected change in decorrelation time results only from the change in the magnitude of the Brownian motion (due to the viscosity change). The different mixtures were then poured into a black plastic container with absorbing walls and size (14 X 9.5 X 7.5 cm^3) that minimize boundary effects.

3. RESULTS

The temporal behavior of coherent light under the influence of different motions within a tissue, i.e. Brownian motion, Blood Flow and US field, was modeled and analyzed in computerized simulation using MATLAB® environment. It was modularly built to enable the user to observe both the effect of each motion separately, as well as the cumulative effect of all of them together (or any desired combination). The final output, as explained before, was the intensity autocorrelation function, from which the decorrelation time can be easily extracted. Figure 3 (left) exemplifies an autocorrelation function calculated by the simulation as a response to Brownian motion. A closer look at the marked region of interest (right) reveals an exponential decay which is consistent with our prediction from the mathematical model (equation (1.7)). The exponential fit is also presented.

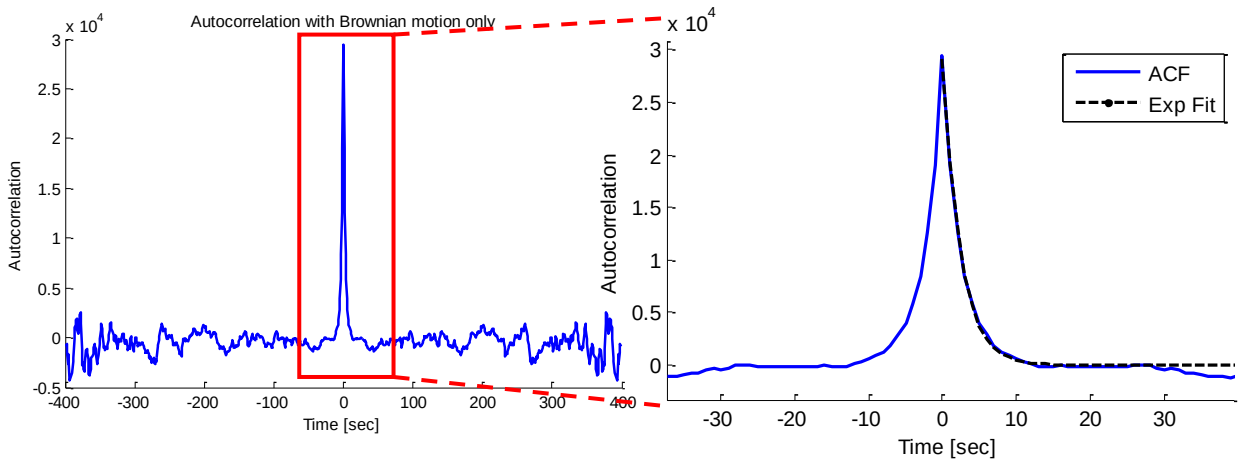

Figure 3: Simulated autocorrelation function for a case of Brownian motion only. On the right there is an enlargement of the marked region of interest which exposes an exponential decay, as expected from theory.

In the case of Brownian motion only, the decay rate is dependent upon the diffusion coefficient which is supplied to the simulation and represents the Brownian motion magnitude in the tissue (equation (1.6)). Figure 4 illustrates two simulated autocorrelation functions, corresponding to two diffusion coefficients $D_1 = 1 \cdot 10^{-15}\, m^2/\text{sec}$ and $D_2 = 1 \cdot 10^{-16}\, m^2/\text{sec}$ ($D_1 = 10 D_2$). The different decay rate is clearly apparent - higher diffusion coefficient produces a faster decay and vice versa.

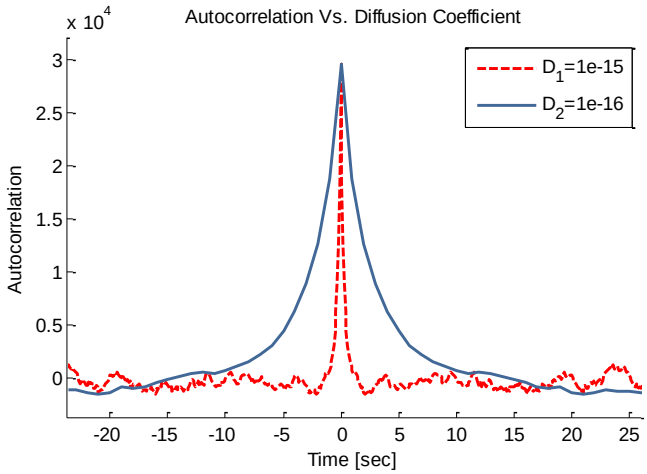

Figure 4: Simulated autocorrelation functions for 2 different diffusion coefficients. Different decay rates are apparent.

In comparison, when the effect of (only) blood flow was investigated using the simulation, a Gaussian decay was observed, as expected from equation (1.11). Figure 5 presents the autocorrelation functions of different velocity magnitudes. One can easily see that the higher the velocity is, the faster the autocorrelation function decays and a shorter decorrelation time is observed.

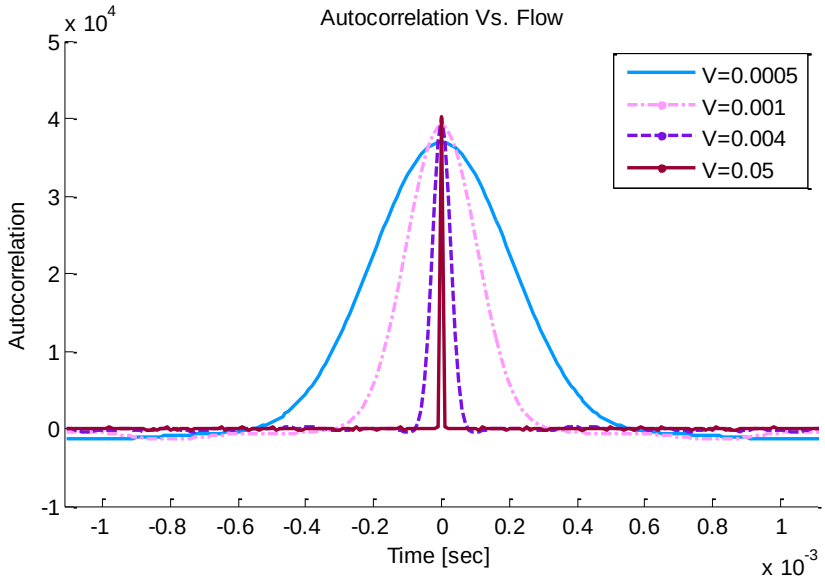

Figure 5: Simulated autocorrelation functions for cases of flow only with different velocity ([m/sec]) magnitudes. A Gaussian shape decay is observed. One can also notice the decay rate dependecy on the velocity magnitue, as expected from theory.

This is in agreement with the known theory of diffused correlation spectroscopy (DCS). When US is combined with the flow, an additional oscillating component accompany the Gaussian decay, as exhibited in Figure 6. The oscillation is at the transmitted US frequency, and its magnitude is determined by the transmitted US magnitude.

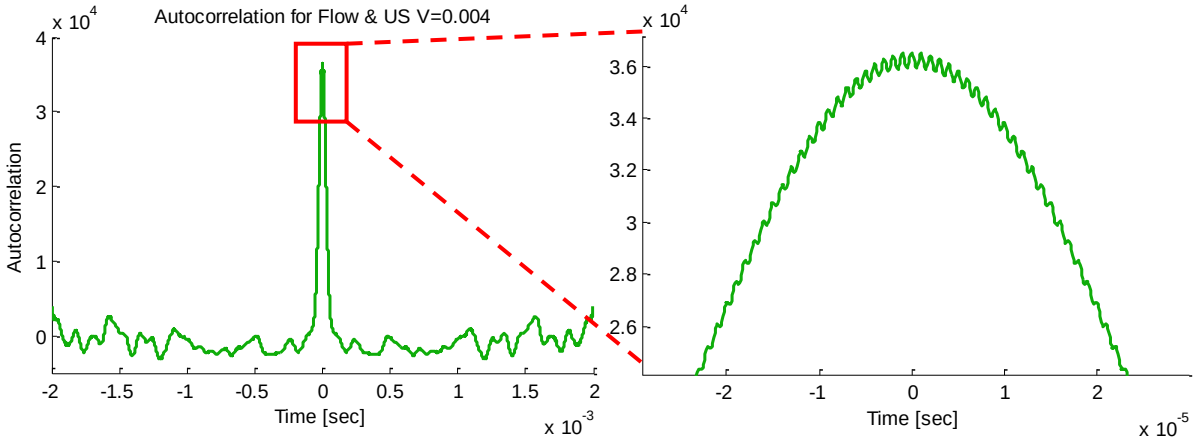

Figure 6: Simulated autocorrelation function for a combined case of flow and US. On the right: an enlargement of the marked region of interest which reveals the additional oscillating component, generated by the US.

Finally, when we apply all of the above mentioned effects together, a combined profile is observed, depending on the ratio between the different parameters, i.e. the diffusion coefficient that determines the Brownian motion magnitude, the blood flow velocity, and the US amplitude and frequency. All these parameters are supplied by the user and can be adapted to model different biological situations.

To validate the simulations' results, the temporal autocorrelation function of different solutions were measured and compared to the simulations' predictions. H_2O-Glycerol solutions were used, at different concentrations, ranging from 80% to 100% glycerol. To obtain a prediction by the simulation, it was supplied with the solution's expected diffusion coefficient, determined by the H_2O-Glycerol composition (which yields the viscosity of the solution) and the Einstein-Stocks equation. Figure 7 exemplifies the autocorrelation function obtained for 90% and 95% Glycerol solutions both by the simulation and the *in-vitro* experiment using the correlator. A similar decay coefficient can be observed, demonstrating a good agreement between the simulation and the measurement.

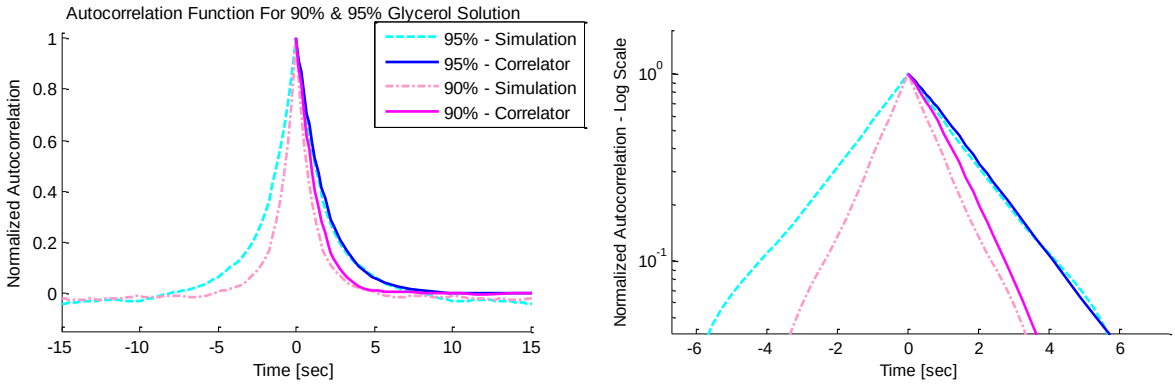

Figure 7: Autocorrelation function for 90% and 95% Glycerol solutions, obtained by both the simulation and the *in-vitro* experiment (Left - linear scale, Right - Log scale). A similar decay can be observed.

Overall performance for 5 different solutions corresponding to 5 different Brownian motion magnitudes is exhibited in Figure 8. Black crosses represent the *in-vitro* experiment results, grey full circles are the simulation's predictions and light grey line is the expected theoretic relation between the two parameters derived from equation (1.7). The number of

scattering events, N, was chosen as twice as the most probable number of scatterers of the trajectories within the medium, obtained by the Monte-Carlo simulation. It is clearly seen that the simulation provided good prediction to the actual measurements.

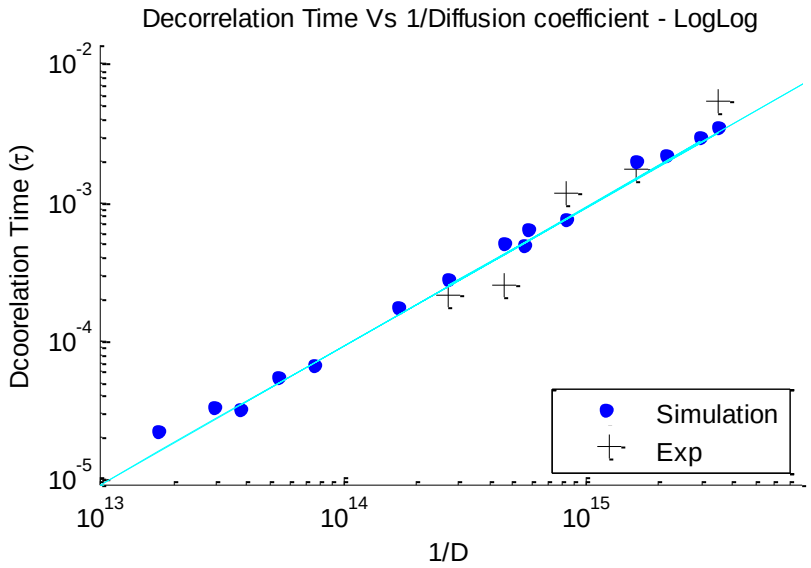

Figure 8: Overall performance of the simulation comparing to the *in-vitro* measurements. A similar behavior and a good correlation to the theory can be seen.

To evaluate the reliability of our simulation, we further applied a regression model with 95% confidence interval (CI) for the simulation's observations (log Decorrelation time (tau) vs. log (1/Diffusion coefficient)). Figure 9 demonstrates that 4 out of 5 experimental points are contained within the 95% confidence interval of the simulation. The other point is also adjacent and practically "touches" the CI as well. This suggests that the simulation can estimate the experimental results accurately. It is a further evidence for the simulation's agreement with the measured values and conclusively proves its good performance.

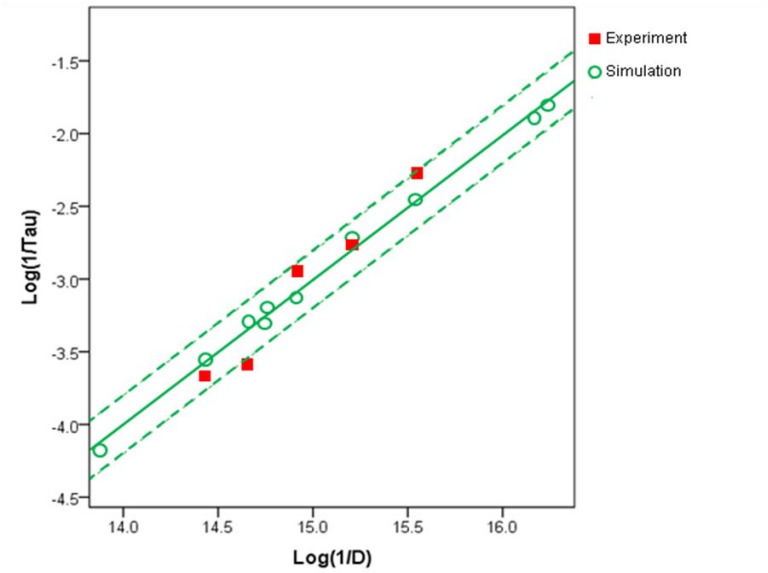

Figure 9: Fit of a regression line (grey line, R^2=0.998) to the simulation's results (grey circles). The grey dashed lines represent the 95% confidence interval. The experimental measurements (dark grey squares) are contained within this interval.

4. DISCUSSION

A novel comprehensive simulation, uniting the effects of Brownian motion, blood flow and US on light transmitted through a tissue, was presented and validated. In general, the simulation exhibited good correlations with both predictions of theory and laboratorial measurements. It suggests that this simulation is indeed useful and might assist in various optical based applications for blood flow measurements and particularly, in methods using the acousto-optic effect.

One possible use, for example, is utilization of this simulation in quantification of non-invasive measurements of blood flow in methods which combine light and US. Previous works, aimed for laser Doppler application, have already shown that blood flow parameters, such as velocity magnitude and the concentration of moving blood cells, can be determined from light intensity spectrum fluctuations[17]. Our simulation expands the observation on light intensity signal with the addition of US effect on it, allowing an insight of the total impact gathered by all existing motions within the tissue. Thus, it might enable isolation of blood flow influence specifically, and deduction of its parameters for US based methods as well.

The proposed simulation was validated in the presence of Brownian motion only. Experiments exhibited good agreement with the simulations predictions. Additional experiments should be carried to further validate its performance in the presence of directional flow and US. Such a comprehensive analysis would enable a complete understanding of its capabilities. It should further permit its usage for flow calibration and quantification.

The validation process was carried using glycerol-water solutions in the range of 80%-100% glycerol only. This range was specifically chosen, as it mimics tissue properties. Lower concentrations will have lower viscosity which makes them irrelevant for this purpose. Furthermore, for different (smaller) glycerol concentrations, the optical properties of the solution might change (the scattering coefficient for example), hence requiring a new set of trajectories, other than the one we used in this work.

Several assumptions were made in this simulation. As previously mentioned, we assumed a constant set of trajectories which are shifted by the existing motions within the tissue. However, it is not clear whether the "perturbed" trajectories are indeed true trajectories, a fact which was neglected in this investigation. We further considered the set of selected trajectories as a single speckle, and thus neglected possible spatial effects involving multiple speckle correlations.

It is also worth mentioning that another possible noise source to the simulation can emanate from the fact that using the MC we get a set of "sampled trajectories", which are only a very small sub-sample of all possible trajectories. It may cause fluctuations in the intensity measured at t=0 for different experiments, and can be reduced as a square root of the number of independent samples. One should define the desired accuracy and select the number of trajectories accordingly.

Additional possible limitation arises from the trajectories selection method. The photons trajectories within the tissue are chosen consecutively, using a Monte-Carlo method. In this process, a photon is emitted, and its trajectory is defined step by step until it reaches the detector. A second photon is then emitted and the procedure is repeated. However, since the parameters of the photon steps within the tissue are randomly selected (step size, angles, etc), photons from different iterations do not interact with the same pattern of scatterers. It's as if the photon is emitted towards another, new medium, having the same optical properties. We assume that since the optical properties between consecutive photons are exactly the same, the influence of such variations is minor.

Finally, a comprehensive simulation was introduced and validated. Its predictions' compliance to *in-vitro* measurements suggests that the approach taken here illustrates well the actual behavior of photons in the presence of motions within a tissue. It is, in fact, a promising first step toward a thorough understanding of ultrasound tagged light nature, and development of tools for blood flow quantification, non-invasively.

5. REFERENCES

[1] H. W. Schytz, S. Guo, L. T. Jensen *et al.*, “A new technology for detecting cerebral blood flow: a comparative study of ultrasound tagged NIRS and 133Xe-SPECT,” Neurocritical care, 17(1), 139-145 (2012).

[2] A. Ron, N. Racheli, I. Breskin *et al.*, "Measuring tissue blood flow using ultrasound modulated diffused light." 8223, 82232J-1.

[3] Q. Zhu, T. Durduran, V. Ntziachristos *et al.*, “Imager that combines near-infrared diffusive light and ultrasound,” Optics letters, 24(15), 1050-1052 (1999).

[4] J. P. Culver, T. Durduran, D. Furuya *et al.*, "Diffuse optical tomography of cerebral blood flow, oxygenation, and metabolism in rat during focal ischemia," Journal of Cerebral Blood Flow & Metabolism, 23(8), 911-924 (2003).
[5] R. Graaff, M. Koelink, F. De Mul *et al.*, "Condensed Monte Carlo simulations for the description of light transport," Applied Optics, 32(4), 426-434 (1993).
[6] L. Wang, S. L. Jacques, and L. Zheng, "MCML—Monte Carlo modeling of light transport in multi-layered tissues," Computer methods and programs in biomedicine, 47(2), 131-146 (1995).
[7] S. L. Jacques, [Monte Carlo modeling of light transport in tissue (steady state and time of flight)] Springer, (2011).
[8] H. Jentink, F. De Mul, R. Hermsen *et al.*, "Monte Carlo simulations of laser Doppler blood flow measurements in tissue," Applied Optics, 29(16), 2371-2381 (1990).
[9] A. Jakobsson, and G. Nilsson, "Prediction of sampling depth and photon pathlength in laser Doppler flowmetry," Medical and biological Engineering and Computing, 31(3), 301-307 (1993).
[10] K. Wardell, A. Jakobsson, and G. E. Nilsson, "Laser Doppler perfusion imaging by dynamic light scattering," Biomedical Engineering, IEEE Transactions on, 40(4), 309-316 (1993).
[11] M. Koelink, F. De Mul, J. Greve *et al.*, "Laser Doppler blood flowmetry using two wavelengths: Monte Carlo simulations and measurements," Applied Optics, 33(16), 3549-3558 (1994).
[12] F. d. de Mul, M. Koelink, M. Kok *et al.*, "Laser Doppler velocimetry and Monte Carlo simulations on models for blood perfusion in tissue," Applied Optics, 34(28), 6595-6611 (1995).
[13] L. V. Wang, "Mechanisms of ultrasonic modulation of multiply scattered coherent light: a Monte Carlo model," Optics letters, 26(15), 1191-1193 (2001).
[14] S. Sakadžić, and L. V. Wang, "Correlation transfer equation for ultrasound-modulated multiply scattered light," Physical Review E, 74(3), 036618 (2006).
[15] S. Sakadžić, and L. V. Wang, "Correlation transfer equation for multiply scattered light modulated by an ultrasonic pulse," JOSA A, 24(9), 2797-2806 (2007).
[16] S. Sakadzic, and L. V. Wang, "Correlation transfer equation for multiply scattered light modulated by an ultrasonic pulse: an analytical model and Monte Carlo simulation." 6437, 64371K-1.
[17] R. Bonner, and R. Nossal, "Model for laser Doppler measurements of blood flow in tissue," Applied Optics, 20(12), 2097-2107 (1981).
[18] D. Boas, and A. Yodh, "Spatially varying dynamical properties of turbid media probed with diffusing temporal light correlation," JOSA A, 14(1), 192-215 (1997).
[19] A. Lev, and B. Sfez, " In vivo demonstration of the ultrasound-modulated light technique," JOSA A, 20(12), 2347-2354 (2003).
[20] L. G. Henyey, and J. L. Greenstein, "Diffuse radiation in the galaxy," The Astrophysical Journal, 93, 70-83 (1941).
[21] W. Leutz, and G. Maret, "Ultrasonic modulation of multiply scattered light," Physica B: Condensed Matter, 204(1), 14-19 (1995).
[22] L. V. Wang, "Mechanisms of Ultrasonic Modulation of Multiply Scattered Coherent Light: An Analytic Model," Physical Review Letters, 87(4), 043903 (2001).
[23] S. Sakadžić, and L. V. Wang, "Ultrasonic modulation of multiply scattered coherent light: an analytical model for anisotropically scattering media," Physical Review E, 66(2), 026603 (2002).
[24] S. Sakadžić, and L. V. Wang, "Modulation of multiply scattered coherent light by ultrasonic pulses: an analytical model," Physical Review E, 72(3), 036620 (2005).
[25] S. Lévêque-Fort, "Three-dimensional acousto-optic imaging in biological tissues with parallel signal processing," Applied Optics, 40(7), 1029-1036 (2001).
[26] A. Ron, N. Racheli, I. Breskin *et al.*, "A tissue mimicking phantom model for applications combining light and ultrasound." 858307-858307-7.
[27] K. Tahir, and C. Dainty, "Experimental measurements of light scattering from samples with specified optical properties," Journal of Optics A: Pure and Applied Optics, 7(5), 207 (2005).
[28] N.-S. Cheng, "Formula for the viscosity of a glycerol-water mixture," Industrial & engineering chemistry research, 47(9), 3285-3288 (2008).